



**CONCURRENT IRON OVERLOAD AND NEOPLASIA IN  
LESCHENAULT'S ROUSETTES (ROUSETTUS  
LESCHENAULTII): A CASE SERIES**

Authors: Snow, Renata, Tse, May, Hill, Fraser, Choi, Yan Ru, Beatty, Julia, et al.

Source: Journal of Zoo and Wildlife Medicine, 55(1) : 235-247

Published By: American Association of Zoo Veterinarians

URL: <https://doi.org/10.1638/2022-0104>

---

BioOne Complete ([complete.BioOne.org](https://complete.BioOne.org)) is a full-text database of 200 subscribed and open-access titles in the biological, ecological, and environmental sciences published by nonprofit societies, associations, museums, institutions, and presses.

Your use of this PDF, the BioOne Complete website, and all posted and associated content indicates your acceptance of BioOne's Terms of Use, available at [www.bioone.org/terms-of-use](https://www.bioone.org/terms-of-use).

Usage of BioOne Complete content is strictly limited to personal, educational, and non - commercial use. Commercial inquiries or rights and permissions requests should be directed to the individual publisher as copyright holder.

---

BioOne sees sustainable scholarly publishing as an inherently collaborative enterprise connecting authors, nonprofit publishers, academic institutions, research libraries, and research funders in the common goal of maximizing access to critical research.

# CONCURRENT IRON OVERLOAD AND NEOPLASIA IN LESCHENAULT'S ROUSETTES (*ROUSETTUS LESCHENAULTII*): A CASE SERIES

Renata Snow, MA, VetMB, MVetSci, MRCVS, May Tse, BVM&S, MRCVS, DACVP, Fraser Hill, BVSc, FANZCVS, Yan Ru Choi, BSc(Hons), Julia Beatty, BSc(Hons), BVetMed, PhD, FANZCVS, FRCVS, and Alessandro Grioni, DMV, MVS, DipACCM, MRCVS

**Abstract:** This case series investigates a cluster of deaths in a captive colony of Leschenault's rousettes (*Rousettus leschenaultii*). Six of seven bats that died between March and September 2021 were diagnosed postmortem with both iron overload (IO) and neoplasia, neither of which have previously been reported in this species. Iron status was assessed via hepatic histopathological grading, hepatic iron concentration, and, in two cases, serum iron concentration. On histopathological grading, all cases had hemochromatosis except one, which had hemosiderosis. Hepatic iron concentrations did not correlate with histopathological grading. Neoplasms in these six bats included hepatocellular carcinoma (HCC; 4), bronchioloalveolar adenocarcinoma (1), pancreatic adenocarcinoma (1), and sarcoma of the spleen and stomach (1). One bat had two neoplasms (HCC and sarcoma of the spleen and stomach). One additional case of HCC in 2018 was identified on retrospective case review. Etiology was investigated to the extent possible in a clinical setting. Nutritional analysis and drinking water testing found oral iron intake within acceptable bounds; however, dietary vitamin C was potentially excessive and may have contributed to IO. Panhepadnavirus PCR testing of liver tissue was negative for all bats. A species-associated susceptibility to IO, as seen in Egyptian fruit bats (*Rousettus aegyptiacus*), is possible. The high incidence of HCC is suspected to be related to IO; other differentials include viral infection. Causes or contributing factors were not definitively identified for the other neoplasms seen but could include age, inherited risk (given a high level of inbreeding), or an oncogenic virus. Pending further research in this species, it is recommended that keepers of Leschenault's rousettes offer conservative amounts of vitamin C and iron (as for Egyptian fruit bats), submit for postmortem examination any euthanized or found dead, and share records of similar cases.

## INTRODUCTION

This case series investigates a cluster of mortality in a captive colony of Leschenault's rousettes (LR; *Rousettus leschenaultii*). Six of seven individuals that died or were euthanized between March and September 2021 were found on necropsy to have both iron overload (IO; either hemosiderosis or hemochromatosis) and neoplasia. Neither IO nor neoplasia has previously been reported in this species.

Hemosiderosis (iron accumulation without associated pathological changes<sup>24,25</sup>) and hemochromatosis (iron storage disease; significant IO with associated tissue damage, e.g. fibrosis and necrosis<sup>24,25</sup>)

have been documented in multiple bat species. Of these, the Egyptian fruit bat (EFB; *Rousettus aegyptiacus*) dominates the literature: the species is commonly kept in captivity, and hemochromatosis is a key cause of morbidity and mortality in captive EFB.<sup>24</sup> Hemochromatosis has also been reported in a straw-colored fruit bat (*Eidolon helvum*)<sup>23</sup> and the long-haired rousette (*Stenonycteris lanosus*, formerly *Rousettus lanosus*),<sup>13</sup> and hemosiderosis is reported in the Indian flying fox (*Pteropus medius*, formerly *Pteropus giganteus*) and the gray-headed flying fox (*Pteropus poliocephalus*).<sup>5</sup> Although some EFB cases have been associated with high dietary iron concentration,<sup>5</sup> in general the reasons for the susceptibility of this species remain unclear.<sup>40</sup> Suggested explanations include high dietary vitamin C concentration resulting in increased iron absorption;<sup>5,12</sup> high capacity for iron absorption as an adaptation to low iron availability in the wild;<sup>12,24</sup> and differences in iron regulation and storage among bat species.<sup>40</sup>

A wide range of neoplasms has been reported in bats. Once again, EFB dominate the literature, with documented neoplasms in this species including bronchioloalveolar adenoma,<sup>8,24</sup> pancreatic carcinoma,<sup>8</sup> hepatocellular carcinoma (HCC),<sup>24</sup> hepatocellular adenoma,<sup>24</sup> cholangiocarcinoma,<sup>24</sup> hepatic

---

From the Fauna Conservation Department, Kadoorie Farm and Botanic Garden, Lam Kam Road, Tai Po, New Territories, Hong Kong SAR, China (Snow, Grioni); City University Veterinary Diagnostic Laboratory, City University of Hong Kong, Kowloon, Hong Kong SAR, China (Tse, Hill); and Centre for Animal Health and Welfare & Department of Veterinary Clinical Sciences, Jockey Club College of Veterinary Medicine and Life Sciences, City University of Hong Kong, Kowloon, Hong Kong SAR, China (Choi, Beatty). Correspondence should be directed to Dr. Snow (renatas@kfbg.org).

Note: This article contains supplemental material found in the online version only.

carcinoid,<sup>24</sup> pulmonary sarcomatoid carcinoma,<sup>29</sup> renal adenocarcinoma,<sup>24</sup> urinary bladder transitional cell carcinoma,<sup>24</sup> mammary adenoma,<sup>24</sup> parathyroid adenoma,<sup>24</sup> basosquamous carcinoma of the wing membranes,<sup>28</sup> sebaceous epithelioma of haired skin,<sup>34</sup> extraskeletal osteosarcoma of the antebrachium,<sup>35</sup> leiomyosarcoma of the duodenum and of the dorsal subcutis,<sup>4,38</sup> fibrosarcoma of the face,<sup>34</sup> anaplastic sarcoma of the shoulder,<sup>34</sup> oral sarcoma,<sup>24</sup> and cutaneous lymphoma.<sup>34</sup> Occasionally, etiological factors have been identified or suggested: a microchip-associated leiomyosarcoma<sup>38</sup> and papillomavirus infection in a case of basosquamous carcinoma.<sup>28</sup> Of relevance to this case series, one retrospective multi-institutional study found that EFB with hemochromatosis were significantly more likely to have HCC than EFB with hepatic hemosiderosis.<sup>24</sup>

Associations between IO and HCC are well documented in humans,<sup>16,26,33</sup> but the exact role iron plays in carcinogenesis is still being determined.<sup>11,19,36</sup> Other conditions that cause, or increase risk of, cirrhosis and HCC (e.g. hepatitis B virus infection, hepatitis C virus infection, and alcohol abuse) have been considered as confounding factors in the study of iron-driven carcinogenesis;<sup>24,26</sup> however, research shows that iron itself is involved in the pathogenesis of those conditions and thus can act as a co-risk factor for HCC.<sup>36</sup> Studies of iron as a potential risk factor for non-hepatic cancer in humans have had conflicting results.<sup>14</sup> Literature on iron status and neoplasia risk is lacking for other species but includes an experimental study in rats, which suggested that dietary IO may be directly hepatocarcinogenic.<sup>1</sup> One retrospective postmortem study identified five cases of hepatocellular neoplasia and three of nonhepatic neoplasia among 37 captive birds of diverse species with hepatic IO; however, neoplasia rates in birds without hepatic IO were not provided for comparison.<sup>45</sup> Another retrospective study, of captive prosimians with hepatocellular neoplasia, found no correlation between liver iron levels and presence or absence of hepatocellular neoplasia.<sup>48</sup> As in humans, potential confounding factors exist. For example, hepadnavirus (hepatitis B-like virus) infections are associated with HCC in rodents in the family Sciuridae.<sup>7</sup> In bats, numerous hepadnaviruses have been discovered, the pathogenic potential of which is unclear.<sup>37</sup>

This case series describes a cluster of six deaths of LR with concurrent IO and neoplasia, plus two pertinent supplementary cases. Relevant gross and microscopic necropsy findings are reported for each bat, followed by results from the subsequent

investigation. The latter include tissue mineral analysis, water testing, nutritional analysis, and hepadnavirus PCR. It is hoped that examination of potential contributors to pathology will enable better management of this species in captivity and identification of areas requiring further study in wild populations.

## CASE REPORTS

### Colony overview

The cases presented are from a captive colony of LR that has existed for 20 yr at Kadoorie Farm and Botanic Garden (KFBG), Hong Kong SAR, China. The founding group of three individuals were casualties of wild local origin that were non-releasable and so were kept for educational display. They bred among themselves until 2015, when the males were castrated. By 2021, the colony consisted of approximately 40 individuals, all captive born, aged 6–18 yr. Owing to uncertainty over some birth dates, and replacement of microchips over the years, most ages are estimates. The bats are housed in a part-outdoor, part-indoor, mixed-species exhibit with several small- to medium-sized passerines. Their diet consists of chopped mixed fruit, commercial fruit bat gel (product code 5M3U, Mazuri Exotic Animal Nutrition, St. Louis, Missouri 63166, USA) and small amounts of Avipro Plus and Arkvits supplements (both from Vetark, Winchester SO23 9SQ, United Kingdom).

Concerns were first raised when two bats (LR1, LR2) died in close succession in March–April 2021 with similar postmortem findings: hepatomegaly on gross examination, and hemochromatosis and neoplasia on microscopy. Subsequent physical examination of the entire colony identified two more individuals (LR3, LR4) with abdominal organomegaly. Following euthanasia, these too were diagnosed with hemosiderosis or hemochromatosis and neoplasia. In September 2021, two further bats (LR5, LR6) were found dead with hemochromatosis and neoplasia. Retrospective review of institutional necropsy records identified only one similar case, an LR euthanized in 2018 (Supplementary Case A [SCA]). Also included for context is the only other LR that died in the same time period as this case series, a geriatric bat euthanized for reasons unrelated to IO or neoplasia, with no antemortem indicators of either disease process (Supplementary Case B [SCB]).

### Investigation overview

KFBG veterinarians performed all antemortem imaging and sampling, conducted gross

necropsies, and collected postmortem tissue samples. In two cases (LR3, LR4), blood for serum iron testing was drawn from the heart under general anesthesia immediately prior to euthanasia. In all cases except SCA, postmortem sampling included most major thoracic and abdominal organs. For SCA, only the liver was sampled at necropsy and no further samples were available.

Tissue samples collected into 10% neutral buffered formalin were sent to City University Veterinary Diagnostic Laboratory, examined macroscopically, and cut into tissue blocks before being processed routinely overnight by standard histopathology methods, embedded in paraffin wax, cut at 4 µm thick, and stained with H&E.

After evaluation, some sections were stained with Masson's trichrome stain to evaluate fibrous tissue, and all abnormal tissue and liver samples were stained with Perls' Prussian blue to highlight iron.

Board-certified veterinary pathologists at City University Veterinary Diagnostic Laboratory reviewed all slides. No specific diagnostic criteria exist for histopathological examination of neoplasia in bats, so diagnostic criteria and classifications of neoplasia in domestic animals were utilized.<sup>6,31,47</sup> Hepatic histological grading for IO (including iron deposition, fibrosis and necrosis) was done following published grading systems previously developed for EFB.<sup>12,24</sup> IO was classified as hemochromatosis where iron deposition was associated with hepatic fibrosis, necrosis (more than 10 necrotic cells per hundred ×400 fields), or both.<sup>24</sup> Cholestasis and biliary hyperplasia were also graded for reference, using, respectively, a scale developed for humans<sup>20</sup> and a scale developed by the authors.

Tissue, serum, and drinking water quantitative iron analyses were performed by external accredited laboratories. Spearman rank correlation coefficient was used to assess monotonic association between hepatic iron concentration and hepatic histological grading score (calculated as the sum of iron deposition, fibrosis, and necrosis scores; not including scores for cholestasis and biliary hyperplasia). Nutritional composition of the bats' diet was calculated manually using data from the gel and supplement manufacturers and (for fruit) publicly available data published by the United States Department of Agriculture<sup>15</sup> and Food Standards Australia & New Zealand.<sup>2</sup>

Panhepadnavirus PCR testing of liver-derived DNA samples was performed for all cases except SCA. DNA was extracted from 10-µm sections of formalin-fixed paraffin-embedded liver tissue using DNeasy Blood & Tissue Kits (Qiagen GmbH,

Hilden 40724, Germany) as described previously.<sup>30</sup> DNA integrity was confirmed by conventional PCR for GAPDH,<sup>3</sup> with all samples generating the expected 80-bp product on gel electrophoresis.

Liver-derived DNA was next investigated using two different nested PCR protocols for hepadnavirus detection. The first used degenerate primers from a previous study<sup>46</sup> that were adapted following alignment of hepadnavirus genomes available in the National Center for Biotechnology Information database (primer HBV-pol-F2\_2 in Supplementary Table 1). Each reaction contained 100–170 ng of template DNA. First-round PCR reactions were performed using DreamTaq™ Hot Start Green DNA Polymerase (Thermo Fisher Scientific, Vilnius 02241, Lithuania), dNTP (Thermo Fisher Scientific) at a final concentration of 200 µM, and primers at a final concentration of 500 nM. Thermal cycling consisted of an initial denaturation at 95°C for 3 min, followed by 35 cycles of denaturation at 95°C for 30 s, annealing at 58°C for 30 s, and extension step at 72°C for 1 min, before a final extension step at 72°C for 10 min. One microliter of the PCR product from the first round was used as template for the second round. The thermal cycling protocol for the second round was identical to that of the first except that the annealing temperature was 59°C. No-template (molecular-grade water) and positive (domestic cat hepadnavirus positive whole-blood-derived DNA) controls were included in all conventional PCR assays. Products were resolved using 1.5% agarose gel electrophoresis.

The second nested panhepadnavirus PCR used primers described previously<sup>44</sup> (Supplementary Table 1) and was carried out as above, except that an annealing temperature of 55°C was used for both rounds.

### Individual case reports

Pertinent historical, antemortem, gross necropsy, and histopathological findings for the six main cases and two supplementary cases are described below. Signalment and key diagnoses are summarized in Table 1. Details of locations and extent of hepatic iron deposition and pathology are presented in Table 2.

*Case 1: LR1, 9 yr, male, died March 2021:* Bat LR1 was found dead in its enclosure. Gross necropsy revealed severe enlargement of the liver, which was diffusely red-black and congested, with prominent rounding of the liver margins and reduced distinction between lobes. The small

**Table 1.** Summary of signalment and key diagnoses for the Leschenault's rousettes (*Rousettus leschenaultii*) in this case series.

Case ID	Sex	Age at death (yr)	D or E, date <sup>a</sup>	Iron overload present? <sup>b,c</sup>	Gross changes to liver present? <sup>c</sup>	Neoplasia present	Attributable cause of death
LR1	M	9	D, Mar 2021	Y	Y	Hepatocellular carcinoma	Hepatocellular carcinoma
LR2	F	6	D, Apr 2021	Y	Y	Exocrine pancreatic adenocarcinoma, with metastases to liver, intestines, and lungs	Exocrine pancreatic adenocarcinoma
LR3	F	8	E, Apr 2021	Y	Y	Hepatocellular carcinoma Sarcoma (stomach, spleen)	Euthanized for presumed neoplasia
LR4	F	5	E, Jun 2021	Y	Y	Hepatocellular carcinoma	Euthanized for polyarthritis
LR5	F	10	D, Sep 2021	Y	Y	Hepatocellular carcinoma	Hepatocellular carcinoma
LR6	F	10	D, Sep 2021	Y	Y	Bronchioalveolar adenocarcinoma, with intravascular metastatic cells in liver	Bronchioalveolar adenocarcinoma
SCA	F	8	E, Sep 2018	U <sup>d</sup>	Y	Hepatocellular carcinoma	Euthanized for presumed neoplasia
SCB	F	17	E, Apr 2021	Y	N	None detected	Euthanized for osteoarthritis

<sup>a</sup> D, died naturally; E, euthanized.

<sup>b</sup> As assessed by histological examination of liver.

<sup>c</sup> Y, yes; N, no; U, unknown.

<sup>d</sup> Insufficient nonneoplastic hepatic parenchyma available for examination.

intestine had extensive intraluminal hemorrhage and a few fibrinous adhesions between intestinal loops.

Histologically, the liver showed changes consistent with an irregular and highly infiltrative HCC. In addition, in the relatively normal parenchyma there was prominent precipitation of diffuse hemosiderin deposition, as well as portal fibrosis, biliary hyperplasia, canalicular bile stasis, and occasional midzonal and periportal individual necrotic hepatocytes associated with iron deposition.

*Case 2: LR2, 6 yr, female, died April 2021:* Bat LR2 presented weak and icteric with abdominal distension. Ultrasound showed a heterogenous, hypoechoic mass occupying most of the abdomen. The bat died minutes later. Necropsy found the mass to be a severely enlarged liver extending three-quarters of the way from the diaphragm to the pelvic inlet, with rounded edges and reduced distinction between lobes. The majority of the liver was dark red and included some poorly defined 10–20-mm-diameter yellow foci, but along the midline of the liver there was a clearly delineated 7–9-mm-wide green zone from the diaphragmatic aspect of the hilar region to the caudal lobe margin. Low numbers of light-yellow nodules ≤5 mm in diameter were present on the peripancreatic mesentery. A moderate serosanguinous peritoneal effusion was also present.

Histological examination revealed an exocrine pancreatic adenocarcinoma effacing the pancreas. Metastatic neoplastic cells were seen throughout the liver as an irregular mass associated with extensive necrosis and hemorrhage, and in the intestinal serosa and lungs as small nodules and intravascular aggregates of up to 100 cells.

Within the nonneoplastic section of the liver were portal fibrosis, biliary hyperplasia, prominent bile stasis, dense precipitates of diffuse hemosiderin deposition, and random occasional individual necrotic hepatocytes associated with hemosiderin deposition.

*Case 3: LR3, 8 yr, female, died April 2021:* A large abdominal mass was palpated in LR3 during physical examination of the whole colony. LR3 was anesthetized with isoflurane in oxygen via mask for imaging, blood sampling, and euthanasia. Radiographs showed a discrete soft tissue radiopacity extending from the cranioventral abdomen to the ilia on the lateral view and causing severe, asymmetrical distension of the abdominal wall on the ventrodorsal view. Ultrasound showed a mixed-echogenicity soft tissue structure occupying most of the abdomen and displacing intestinal loops. Blood was drawn for serum iron testing (see

**Table 2.** Measures of iron status in Leschenault's rousettes: 1) serum iron concentration in blood drawn immediately prior to euthanasia, 2) mineral analysis of postmortem liver samples, and 3) visual histological grading of postmortem liver samples.

Case ID	Serum iron		Hepatic iron concentration <sup>a</sup>					Hepatic histological grading <sup>b</sup>					Biliary hyperplasia <sup>g</sup>	Hemochromatosis present? <sup>h</sup>
	( $\mu\text{mol/L}$ )	mmol/kg	mg/kg or ppm wet weight	mg/kg or ppm dry weight	Hepatocytes <sup>c</sup>	Kupffer cells <sup>c</sup>	Portal tracts <sup>c</sup>	Biliary epithelium <sup>c</sup>	Fibrosis <sup>d</sup>	Necrosis <sup>d</sup>	Cholestasis <sup>f</sup>			
LR1	ND <sup>i</sup>	49.9	2,786.7	9,196.0	2	3	2	1	2	2	2	2	Y	
LR2	ND	16.7	932.6	3,077.6	3	3	2	1	2	2	3	2	Y	
LR3	21.4	18.6	1,038.7	3,427.8	2	3	2	1	0	1	1	1	N	
LR4	105.5	26.7	1,491.1	4,920.5	3	2	3	3	3*	3	1	3	Y	
LR5	ND	6.0	335.1	1,105.7	3	2	3	3	3*	3	3	3	Y	
LR6	ND	35.8	1,999.3	6,597.5	3	3	3	1	3	3	0	2	Y	
SCB	ND	18.7	1,044.3	3,446.2	3	3	2	1	0	2	2	0	Y	

<sup>a</sup> Mineral analysis results were originally reported in mmol/kg wet weight (with a 95% confidence interval of  $\pm 0.16$  mmol/kg at 3.8 mmol/kg). They have been converted to mg/kg and multiplied by a conversion factor of 3.3 to obtain an approximate dry matter iron concentration.<sup>25</sup>

<sup>b</sup> Histological grading was performed based on previously published methods.<sup>12,24</sup> Scores for cholestasis<sup>20</sup> and biliary hyperplasia (authors' own scale) are also provided for reference.

<sup>c</sup> Key: 0, no iron staining; 1, few iron-stained cells; 2, moderate to numerous iron-stained cells or (in portal tracts) there are iron-stained cells forming occasional small aggregates and occasional small amounts of extracellular iron; 3, most cells contain iron or (in portal tracts) there are coarse irregular intra- and extracellular clumps of iron. Portal tracts include macrophages, fibroblasts, and connective tissue.

<sup>d</sup> Key: 0, minimal connective tissue; 1, fibrous connective tissue equal to width of one hepatocyte in portal regions; 2, fibrous connective tissue greater than or equal to width of two hepatocytes in portal regions; 3, bridging fibrosis. Cases with cirrhosis (bridging fibrosis and regenerative nodules) are marked with an asterisk in this column.

<sup>e</sup> Key: 0, no necrosis; 1, 1–10 necrotic cells per hundred  $\times 400$  fields; 2, 11–20 necrotic cells per hundred  $\times 400$  fields; 3, >20 necrotic cells per hundred  $\times 400$  fields.

<sup>f</sup> Key: 0, none; 1, intrahepatic and/or canalicular bile pigments identified only after careful search under high magnification; 2, intrahepatic and/or canalicular bile pigments not immediately evident at low magnification but easily found at high magnification; 3, intrahepatic and/or canalicular bile pigments easily found at low magnification.

<sup>g</sup> Key: 0, none; 1, one or a few extra small bile ducts in occasional portal tracts; 2, one to multiple small bile ducts in up to 50% of the portal tracts; 3, multiple small bile ducts in most of the portal tracts.

<sup>h</sup> Hemochromatosis diagnosed where necrosis (greater than 10 necrotic cells per hundred  $\times 400$  fields), fibrosis, or both are present and associated with iron deposition.

<sup>i</sup> ND, not done.

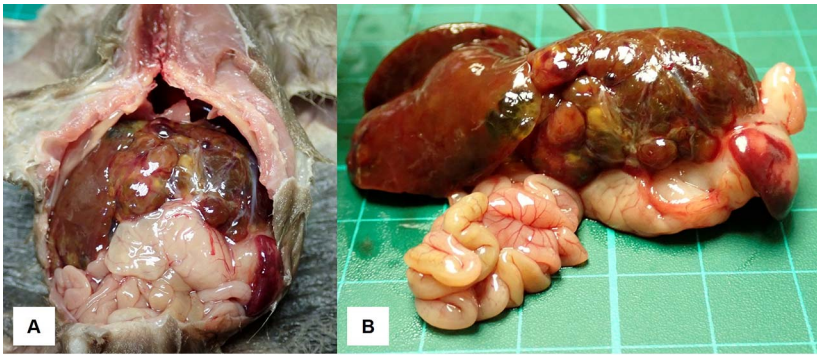


**Figure 1.** Gross necropsy photographs of a Leschenault's rousette (*Rousettus leschenaultii*; patient ID LR3). **A.** Liver in situ, extending halfway from the diaphragm to the pelvic inlet. **B.** Liver, spleen, stomach, and intestines of LR3 after removal from the abdominal cavity. The liver was diffusely enlarged. One lobe (indicated by forceps) was multinodular and mottled tan, brown, and red. The spleen (right of image) had a well demarcated pale pink area, and was adhered to the stomach. (Image credit: Kadoorie Farm and Botanic Garden).

“Iron quantification” below) immediately prior to euthanasia.

On necropsy, the liver was enlarged, extending half of the way from the diaphragm to the pelvic inlet (Fig. 1A). Low numbers of 2–3-mm-diameter, yellow–brown foci were present near the margins bilaterally. One lobe was multinodular and mottled tan, brown, and red (Fig. 1B) and had a caseous consistency on cut section. The dorsal pole of the spleen was adhered to the body wall by a band of white, fibrous tissue, and the ventral pole had a focal region of pale pink tissue adhered to the stomach. The stomach wall was diffusely white, thickened, and firm.

Histological examination of the stomach identified a tumor composed of neoplastic spindle cells consistent with a sarcoma expanding the muscularis, submucosa, and mucosa. The overlying gastric mucosa was focally ulcerated. Similar neoplastic spindle cells were found replacing the parenchyma of the spleen.

In the liver, histological changes were consistent with HCC (Fig. 2). The tumor was multifocally distorted by bands of fibrous tissue and multifocal, randomly distributed areas of coagulative necrosis.

In the remaining parenchyma, there was diffuse deposition of hemosiderin.

**Case 4: LR4, 5 yr, female, died June 2021:** During the same screening that detected LR3, a much smaller abdominal mass was palpated in LR4. LR4 was anesthetized for further workup; the mass was not visible on radiographs, but a 1.08 × 0.81-cm hypoechoic structure was seen in the cranial abdomen on ultrasound. Because the mass was small and the bat was otherwise clinically normal, veterinary staff elected to reassess in 1 mon, with the keepers to monitor closely in the meantime (fur on

the bat's shoulders was bleached to facilitate identification). At reexamination, no abdominal mass could be found on palpation, radiographs, or ultrasound. However, the distal interphalangeal joint of digit III of the left forelimb was noted to be swollen and erythematous. The bat was hospitalized and prescribed a course of amoxicillin clavulanate (Glaxo Wellcome Production, ZI de la Peyrenière, Mayenne 53100, France; 21.5 mg/kg PO q12h) and meloxicam (Boehringer Ingelheim, North Ryde, New South Wales 2113, Australia; 0.3 mg/kg PO q12h). Over the next week, the interphalangeal joints of digit III of the right forelimb also became swollen and abraded, and the swollen joints began to exude serous liquid. The bat was anesthetized and blood was drawn for serum iron testing immediately prior to euthanasia.

On necropsy, the liver was dark red with three to four poorly defined 10-mm-diameter yellow–brown foci, one of which was gray and fibrous on cut section.

Histological examination revealed HCC. In the rest of the liver, there was diffuse hemosiderin deposition, biliary hyperplasia, portal infiltrates of large numbers of hemosiderin-laden macrophages and fewer lymphocytes and neutrophils, and portal fibrosis with multifocal extensive bridging fibrosis associated with regenerative nodules, consistent with cirrhosis. Centrilobular and midzonal hepatocytes in small to moderate groups, and to a lesser extent periportal hepatocytes, were often necrotic and associated with hemosiderin deposition.

Histopathology of the connective tissue surrounding the interphalangeal joint identified moderate, necrotizing, neutrophilic and histiocytic cellulitis, without cartilage or bone involvement but with ulceration, epidermal hyperplasia, intralesional

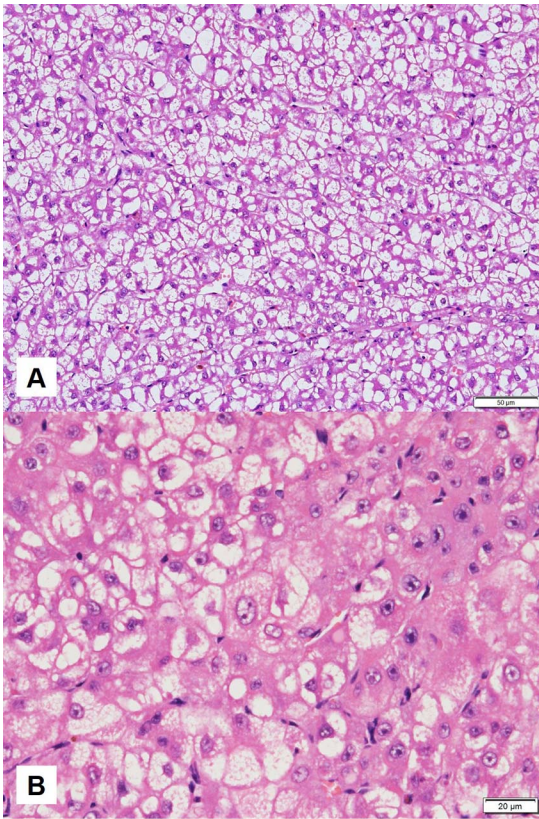


**Figure 2.** Histopathology (H&E stain) of the liver from a Leschenault's rousette (*Rousettus leschenaultii*; patient ID LR3). **A.** The abnormal liver was composed of neoplastic cells resembling hepatocytes forming disorganized hepatic cords of up to 20 cells thick. **B.** A higher magnification of (A) showing marked anisokaryosis and anisocytosis among neoplastic cells. (Image credit: CityU VDL).

free hair shafts, and surface yeasts with similar morphology to *Malassezia* sp. organisms.

**Case 5: LR5, 10 yr, female, died September 2021:** Bat LR5 was found dead. Necropsy revealed 2–4-mm-diameter, spherical masses throughout the liver, replacing most of the normal liver tissue. The liver had patchy yellow, tan, and green discoloration.

On histological examination, approximately 60% of examined sections of the liver parenchyma was replaced by HCC. In the rest of the parenchyma the connective tissue of medium and large portal tracts often had small to large numbers of hemosiderin-laden macrophages, fewer lymphocytes, and occasional neutrophils, as well as fibrosis. Frequent extensive bridging fibrosis separated the regenerating hepatic parenchyma, consistent with cirrhosis. Cholestasis was present. Multifocal random clusters

of necrotic hepatocytes were associated with replacement hemorrhage, neutrophils, and lymphocytes. There was diffuse hemosiderin deposition associated with frequent individual necrotic hepatocytes.

**Case 6: LR6, 10 yr, female, died September 2021:** Bat LR6 was found dead. On necropsy, the left side of the liver had a lobulated mass, of which one lobule was tan and firm and the other lobules were red to black and friable. There was a moderate left-sided hemothorax. Three 2–5-mm-diameter red to black masses were present on the pericardium and in the lungs.

On histological examination, expanding, replacing, and compressing the normal pulmonary parenchyma were multiple foci of bronchioloalveolar adenocarcinoma composed of neoplastic polygonal to cuboidal cells forming acinar and papillary structures supported by a fine fibrovascular stroma. Within the neoplasm were variable areas of congestion, hemorrhage, fibrin precipitates, and coagulative necrosis. Neoplastic cells extended into the lumen of airways and onto the pleural surface.

In the liver, bronchioloalveolar adenocarcinoma emboli were visible in the lumen of two major veins with confluent necrosis involving all zones in one of the lobules. The connective tissue of portal tracts often had a small to moderate infiltrate of hemosiderin-laden macrophages and a few lymphocytes, on a background of portal fibrosis with occasional extensive bridging fibrosis (Fig. 3). There were occasional individual necrotic hepatocytes and rare small groups of periportal necrotic hepatocytes associated with diffuse hemosiderin deposition.

**SCA: 8 yr, female, died September 2018:** This case was identified retrospectively; only basic gross necropsy records, slides of liver sections, and the original hepatic histopathology report were available for reference. The bat initially presented for failure to fly but physical examination found no significant abnormalities. Empirical treatment with meloxicam (0.2 mg/kg PO q24h) and rest was unsuccessful. Two weeks later, icterus and abdominal distension were noted and the bat was euthanized. Gross necropsy revealed hepatomegaly, including one large multilobular intrahepatic mass along with multifocal green hepatic nodules.

Histological examination revealed HCC in the liver. Within the neoplasm there was frequent canalicular cholestasis and occasional random, moderate to large areas of necrosis. Kupffer cells within the minimal, highly compressed, remnant hepatic parenchyma were filled with hemosiderin.

**SCB: 17 yr, female, died April 2021:** During the same time period as Cases 1–6, this geriatric

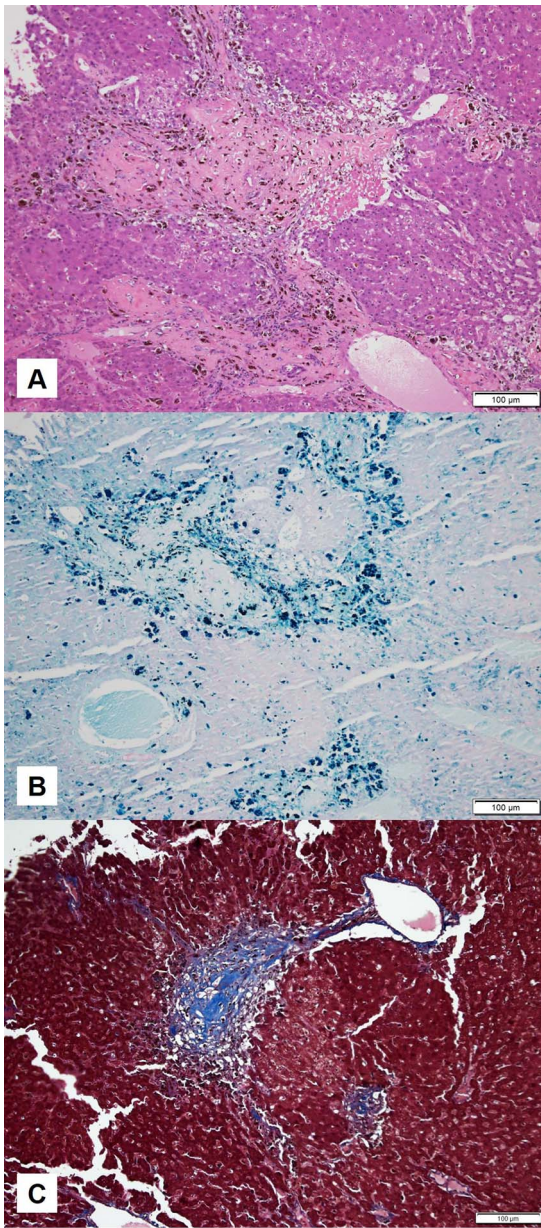


**Figure 3.** Histopathology (H&E stain, Perls' Prussian blue stain, and Masson's trichrome stain) of the liver from a Leschenault's rousette (*Rousettus leschenaultii*; patient ID LR6). **A.** The portal tract connective tissue was variably expanded by fibrosis with biliary proliferation, brown pigment-laden macrophages, and occasional individual to groups of necrotic hepatocytes. The portal fibrosis extended to the neighboring portal tract. **B.** Perls' Prussian blue stain of (A) highlights iron-stained (blue) macrophages denser in the portal tracts, hepatocytes, and Kupffer cells. **C.** Masson's trichrome stain of (A) highlights the collagen bundles in the portal tract. (Image credit: CityU VDL).

bat was found on the ground. It was euthanized after radiographs found severe osteoarthritis of multiple joints (including both shoulders, the proximal and middle interphalangeal joints of digit III of the left forelimb, and the proximal and distal interphalangeal joints of digit III of the right forelimb), as well as moderate ventral spondylosis deformans of T11–T12, T12–T13, L2–L3, L3–L4 and L4–S1. On necropsy, the lungs were congested and had white-tan margins (which histological examination found most likely to be lipid and an age-related change). The internal organs were otherwise grossly normal.

On histological examination of the liver, rare random hepatocytes contained macrovesicular lipid vacuoles. Occasional individual necrotic hepatocytes were scattered through the hepatic parenchyma with increased numbers of necrotic cells around portal areas, associated with diffuse hemosiderin deposition. Unlike the other bats in this case series, SCB had no gross or histological evidence of neoplasia.

#### Iron quantification

The first cases in this cluster raised concerns regarding iron status, so efforts were made to quantify the degree of overload. Quantification was not possible for retrospective case SCA, because no archived tissue samples were available and there was insufficient remnant hepatic parenchyma for full histological grading.

**Serum iron testing:** This was performed in two cases, LR3 and LR4, with results of 21.4  $\mu\text{mol/L}$  and 105.5  $\mu\text{mol/L}$  respectively.

**Mineral analysis:** Liver iron concentrations ranged from 6.0 to 49.9 mmol/kg wet weight (Table 2), approximately equivalent to 1,105.7–9,196.0 mg/kg dry weight.

**Hepatic histological grading:** Histological grading for degree of iron deposition, fibrosis, and necrosis was performed (Table 2). All seven bats assessed had moderate to large amounts of iron deposition within parenchymal cells and Kupffer cells, followed by portal tract macrophages or as extracellular aggregates in portal tracts, and in biliary epithelium, in decreasing severity. Hemochromatosis (fibrosis and/or necrosis associated with iron deposition) was identified in six of the seven. In the remaining bat, LR3, only hemosiderosis was present.

There was no statistically significant monotonic association between hepatic iron concentration and total histological grading score ( $r_s = -0.108$ ,  $n = 7$ ,  $P = 0.818$ ).

### Water testing

Iron concentrations in the bats' drinking water were 0.04 mg/L (indoor tap) and 0.06 mg/L (outdoor tap). As obligate frugivores, the bats likely consume most of their water through the fruit they eat,<sup>21</sup> but wild LR have been observed drinking water directly (Tsui, pers. comm.). For the sake of argument, assuming the highest bat drinking water intake found in the literature (21% of body weight per day, in lactating insectivorous bats,<sup>22</sup> likely to be a vast overestimate for this LR colony), LR in this case series would consume up to 0.001 mg iron per bat per day (0.013 mg/kg per day) in their water.

### Nutritional analysis

Nutritional analysis was limited by multiple factors beyond the authors' control. These included 1) lack of resources and local capacity for direct laboratory analysis of food offered; 2) lack of recently published data representative of the types of fruit fed and the geographical ranges from which they were imported; 3) wide variation in the types and relative proportions of fruit fed and the geographical areas from which they were imported, depending on season, cost, and availability; 4) lack of recorded information on exact proportions and geographical origins of fruit fed over the preceding months and years; 5) normal LR feeding behavior in which juice is consumed but fiber left behind; and 6) individual variation in fruit consumption. However, because diet is a key potential contributor to IO, it was considered important to obtain at least a ballpark estimate of iron and vitamin C content, in order to gauge the likelihood of inadvertent overprovision.

Calculations were performed under different sets of assumptions for comparison. Assumptions included 1) that all 13 fruits on the current animal feed shopping list were offered in equal amounts and consumed in equal amounts; 2) that only the five most commonly and consistently fed fruits (guava, banana, papaya, apple, pear) were offered, and offered and consumed in equal amounts; 3) that 100% of food offered was consumed; and 4) that only 25% of fruit micronutrients offered were consumed (the same "conservative estimate" used by other authors to account for fruit bat feeding behavior<sup>12</sup>).

Although the specific figures thus obtained should be considered loose estimates, a few key findings did emerge from this process. Fruit was the major source of vitamin C, with gel and supplements providing negligible amounts in comparison.

Assuming 100% consumption, the estimated total daily vitamin C intake was up to 101.92 mg/bat per day (1,098.30 mg/kg per day). Guava, a commonly fed fruit, was a major contributor: of all the fruits available, guava had by far the highest vitamin C content (228.3 mg/100 g; the next highest was kiwifruit at 74.7 mg/100 g<sup>15</sup>). Fruit and gel were the major sources of dietary iron, with supplements and drinking water contributing small to negligible amounts. Assuming 100% consumption of food offered, and a very high intake of drinking water (21% of body weight per day; see above), the maximum estimated total iron intake was up to 0.67 mg/bat per day (7.20 mg/kg per day).

Lower-end estimates, assuming consumption of 25% of fruit micronutrients offered and 5% of body weight per day in drinking water, were 19.27–26.26 mg/bat per day (207.70–283.00 mg/kg per day) for vitamin C and 0.37–0.38 mg/bat per day (3.91–4.04 mg/kg per day) for iron.

### Viral testing

PCR products of the expected size were generated in the positive control samples, but not in the liver-derived DNA samples or in the negative control samples, indicating that all liver-derived DNA samples tested negative for hepadnavirus sequences.

## DISCUSSION

### Assessing IO

Histopathological examination in this case series found hemochromatosis to be common, but in contrast to previous work<sup>12</sup> there was no correlation between hepatic histological grading and hepatic iron concentration, and quantitative measurement of hepatic iron concentrations did not show the degree of overload expected. Normal hepatic iron concentrations have not been published for LR; however, previous studies of EFB have defined IO as more than 3 SDs above the mean hepatic iron concentration reported in wild EFB (i.e. iron concentrations above 940.3 mg/kg wet weight in males and 1,780.2 mg/kg wet weight in females).<sup>12,40,43</sup> Using the same criteria, only two bats in this case series, LR1 and LR6, would be considered as having IO. All bats had iron concentrations below the previously suggested toxicity threshold in EFB of 12,000 mg/kg dry weight.<sup>5</sup>

There are reasons why histological grading might not correlate with hepatic iron concentrations. Variations in iron deposition within the liver could affect measured concentrations, depending on which region was sampled: neoplastic areas and regenerative nodules often contain less iron than

remnant parenchyma. In addition, a statistically significant relationship (if one exists) is unlikely to be found with a sample size of seven.

As for serum iron measurement, normal LR serum iron values are unknown; however, the serum iron of LR3 was similar to the reported mean for EFB with normal iron status whereas that of LR4 was almost double the mean of EFB with hemochromatosis.<sup>12</sup> Again, the small sample size precludes any judgment of the significance of these results, and further studies are needed.

### Causes of IO

Of the numerous reported causes (or potential causes) of hepatic IO in the literature, the following three are considered most plausible for these LR and are discussed further below: a species-associated susceptibility, a hereditary iron storage disorder, and diet. Infection is another possible, but less likely, differential: although panhepadnavirus PCR testing was negative, other viruses not tested for could interfere with iron homeostasis. For example, hepatitis C virus (a flavivirus) infection in humans first upregulates, then downregulates hepcidin expression, ultimately leading to IO.<sup>36</sup> However, such a mechanism has not to our knowledge been reported in animals, and histological findings in these bats did not suggest concurrent infection. Other differentials for IO were not supported by the patients' history (e.g. transfusions<sup>10</sup>), gross findings (e.g. cachexia<sup>18</sup>), or histological findings (e.g. chronic hepatitis, chronic renal disease, systemic inflammatory processes<sup>10,25</sup>).

A species-associated susceptibility to IO, similar to that seen in EFB, is possible, and could exist as an adaptation to dietary or environmental factors similar to those faced by EFB. The underlying genetics require further study: EFB appear limited in their ability to upregulate hepcidin expression in response to iron challenge,<sup>40</sup> but in comparisons with other bat species, no significant differences were found in the hepcidin gene itself<sup>39</sup> and little is known about the activity of other proteins and genes involved in iron regulation in *Rousettus* spp.

Also possible is some type of hereditary iron storage disorder made phenotypically apparent by the high level of inbreeding in this colony.

Finally, problems with the captive diet are a key differential; IO has been attributed to excessive dietary iron and vitamin C in the captive EFB literature.<sup>5</sup> The remainder of this section will therefore examine differences between wild and captive LR diets, and potential issues with the latter.

A handful of studies have been published on LR feeding habits in various parts of their natural range. Notable differences in reported wild diets compared with the diet offered to captive LR in this case series include a greater dependency on wild fruits (although commercially grown fruits are also consumed in the wild); fruits of the families Moraceae (e.g. fig) and Sapindaceae (e.g. rambutan, lychee, longan) constituting a large proportion of the diet; guava being consumed for part of the year rather than the whole year; and small amounts of leaves, nectar, and other plant parts being consumed in addition to fruit.<sup>41,42</sup> Further study of the nutritional implications of these differences could help shed light on issues of iron homeostasis; for example, it has been hypothesized that EFB may naturally consume inhibitors of iron absorption such as tannins.<sup>12</sup>

However, for now, data on normal ranges of iron and vitamin C intake for wild LR are not available. Analysis in this captive setting was limited by the six factors outlined earlier in this paper, and both wild LR and this captive colony would benefit from a proper dietary study. Nonetheless, attempts were made to estimate intake, in order at least to gauge the likelihood of overprovision.

The conservative (high end) estimated iron intake of up to 0.67 mg/bat per day was well below the 5 mg/bat per day documented in a previous case of overdose in EFB<sup>5</sup> (note that EFB are similar to, to double LR in mass). It is generally recommended that species prone to hemochromatosis be fed less than 100 ppm iron;<sup>23</sup> in this LR colony, the conservative (high end) estimated total iron content of 36 ppm dry matter (combined fruit and gel) was well below that. It is possible that actual iron concentrations were higher: although biochemical analysis was not possible in this case, previous studies report that laboratory-analyzed iron content can be significantly higher than the calculated content.<sup>23</sup> However, it is also possible that actual iron concentrations were lower: studies from both the United States and the United Kingdom have shown a reduction in fruit iron content over the 20th century<sup>9,27</sup> and the source data for dietary estimates in this paper are decades old. In the absence of accurate figures, it may be worth noting that the LR share an enclosure with two species in the family Sturnidae (*Gracupica nigricollis* and *Acridotheres cristatellus*); birds in the enclosure have access to a similar selection of fruit and have been observed feeding from the bats' bowls too. Sturnidae have a known predisposition to IO, but this institution has not observed IO or clinical illness in these birds. Overall, based on the limited

information available, although iron overprovision cannot be ruled out, it appears to be a less likely cause for the IO seen in this bat colony.

In contrast, the estimated dietary vitamin C content of 5,473 mg/kg dry matter was extremely high; intake estimates ranged from 19.27–26.26 mg/bat per day (low end) to 73.97–101.92 mg/bat per day (high end). This was largely due to the inclusion of guava, a fruit favored for being locally grown and relatively cheap. By way of comparison, EFB were offered approximately 18–24 mg/d in a previous study<sup>12</sup> and were estimated to consume 90 mg/d in a previous hemochromatosis case series.<sup>5</sup> (For further comparison, the human adult recommended daily allowance is 75–90 mg, depending on sex, or approximately 1 mg/kg.<sup>32</sup>)

Thus, using the EFB literature as a guide, dietary vitamin C concentrations appear potentially excessive and more likely to be a problem than dietary iron concentrations in this colony. Vitamin C is known to increase iron absorption and potentiate iron toxicity,<sup>5</sup> and so excessive vitamin C could increase the risks associated with an apparently acceptable iron intake.

### Neoplasia

This case series was characterized by an assortment of neoplasia, most commonly HCC. As previously discussed, hepatic IO has been associated with HCC in humans and EFB.<sup>24</sup> A suitable control group of LR is not available for comparison, but it is plausible (and perhaps most likely) that IO may account for the high prevalence of HCC seen here. Viral infection, for example hepatitis B virus (a hepadnavirus) and hepatitis C virus in humans, can also increase HCC risk through a range of different mechanisms, but often as a sequel to cirrhosis.<sup>36</sup> Although panhepadnavirus testing was negative in these LR, other oncogenic viruses have not been ruled out. Chronic aflatoxicosis is another risk factor for HCC in humans<sup>17</sup> but is less likely in these bats because 1) their diet does not contain foodstuffs typically associated with aflatoxins and 2) insofar as lesions seen in domestic species can be extrapolated to bats, certain histopathological signs of aflatoxicosis (e.g. megalocytosis) were absent in these LR. Other mycotoxins have not been ruled out; however, not enough information is available (either on exposure to specific mycotoxins or on the effects of mycotoxins in this species) to be able to assess the validity of this differential.

As for nonhepatic neoplasia, the existing literature does not support a relationship with IO, raising the question of what else might be causing the

high prevalence of neoplasia in these bats. Possibilities include inherited risk factors (especially given the high level of inbreeding), oncogenic viruses, or some bats being older than thought.

Of note, to date such problems with IO and neoplasia have not been seen in the other bat colony (short-nosed fruit bats; *Cynopterus sphinx*) maintained on the same diet at the same institution. No published data exist on causes of morbidity or mortality in captive LR elsewhere, likely because the species is uncommonly kept in zoological collections.

### CONCLUSIONS

This case series represents the first report of IO and neoplasia in *R. leschenaultii*. This captive colony showed a pattern of IO and HCC reminiscent of that widely seen in captive EFB; three extrahepatic neoplasms were also identified. The cause of IO, as with EFB, is unclear: it may be due to a species-associated adaptation of iron homeostasis and/or to differences in the captive diet relative to the wild diet. Concerns specific to this colony include a high vitamin C intake and high levels of inbreeding. HCC is suspected to be related to IO, but other differentials exist. Although panhepadnavirus infection was largely ruled out, infection by other oncogenic viruses is possible, as is an inherited cancer risk.

Pending further investigation, it is recommended that keepers of captive LR feed conservative amounts of vitamin C and iron (as for EFB), avoid inbreeding, and perform routine necropsies of bats found dead or euthanized, sharing records of any similar cases. Future research should aim to fill the large gaps in the literature for this species, including nutritional analysis of wild diets, normal iron parameters of wild LR, behavior of proteins involved in iron regulation, methods for assessing iron status, and further viral testing.

*Acknowledgments:* The authors thank Ms. Debbie Ng, Mrs. Amanda Crow, and Dr. Gary Ades at Kadoorie Farm and Botanic Garden; Dr. Jeanine Sandy and Dr. Andrew Ferguson at City University; Ms. Wing Tsui, Mr. Pierce Lai, Dr. Meredith Wall, and Dr. Virginie De Busscher; and the two anonymous reviewers of this manuscript. The work described in this paper was supported by the Kadoorie Farm and Botanic Garden veterinary hospital budget, City University Veterinary Diagnostic Laboratory, and a grant from City University of Hong Kong to Beatty (Tumor Virology Program, Project No. 9380111).

## LITERATURE CITED

1. Asare GA, Paterson AC, Kew MC, Khan S, Mossanda KS. Iron-free neoplastic nodules and hepatocellular carcinoma without cirrhosis in Wistar rats fed a diet high in iron. *J Pathol.* 2006;208(1):82–90.
2. Australian food composition database. Food Standards Australia & New Zealand [Internet]. 2022. <https://www.foodstandards.gov.au/science/monitoringnutrients/afcd/Pages/default.aspx>
3. Beatty JA, Troyer RM, Carver S, Barrs VR, Espinasse F, Conradi O, Stutzman-Rodriguez K, Chan CC, Tasker S, Lappin MR, VandeWoude S. *Felis catus* gammaherpesvirus 1; a widely endemic potential pathogen of domestic cats. *Virology.* 2014;460–461:100–107. 10.1016/j.virol.2014.05.007.
4. Bradford C, Jennings R, Ramos-Vara J. Gastrointestinal leiomyosarcoma in an Egyptian fruit bat (*Rousettus aegyptiacus*). *J Vet Diagn Invest.* 2010;22(3):462–465.
5. Crawshaw G, Oyarzun S, Valdes E, Rose K. Hemochromatosis (iron storage disease) in fruit bats. In: Proc Am Zoo Aquat Assoc Nutr Advis Group; 1995. <https://nagonline.net/891/hemochromatosis-iron-storage-disease-fruit-bats/>
6. Cullen JM. Tumors of the liver and gallbladder. In: Meuten DJ (ed.). *Tumors in domestic animals.* 5th ed. Ames (IA): John Wiley & Sons, Inc; 2017. p. 602–631.
7. Cullen JM, Lindsey-Pegram D, Cote PJ. Serologic survey of woodchuck hepatitis virus in North Carolina woodchucks (*Marmota monax*). *J Zoo Wildl Med.* 2008;39(2):263–265.
8. Cushing AC, Ossiboff R, Buckles E, Abou-Madi N. Metastatic pancreatic carcinoma and bronchioloalveolar adenomas in an Egyptian fruit bat (*Rousettus aegyptiacus*). *J Zoo Wildl Med.* 2013;44(3):794–798.
9. Davis DR, Epp MD, Riordan HD. Changes in USDA food composition data for 43 garden crops, 1950 to 1999. *J Am Coll Nutr.* 2004;23(6):669–682.
10. Deugnier Y, Turlin B. Pathology of hepatic iron overload. *World J Gastroenterol.* 2007;13(35):4755–4760.
11. Fargion S, Valenti L, Fracanzani AL. Role of iron in hepatocellular carcinoma. *Clin Liver Dis (Hoboken).* 2014;3(5):108–110.
12. Farina LL, Heard DJ, LeBlanc DM, Hall JO, Stevens G, Wellehan JFX, Detrisac CJ. Iron storage disease in captive Egyptian fruit bats (*Rousettus aegyptiacus*): relationship of blood iron parameters to hepatic iron concentrations and hepatic histopathology. *J Zoo Wildl Med.* 2005;36(2):212–221.
13. Farina LL, Lankton JS. Chiroptera. In: Terio K, McAloose D, St. Leger J (eds.). *Pathology of wildlife and zoo animals.* 1st ed. Elsevier; 2018. p. 607–633.
14. Fonseca-Nunes A, Jakszyn P, Agudo A. Iron and cancer risk—a systematic review and meta-analysis of the epidemiological evidence. *Cancer Epidemiol Biomarkers Prev.* 2014;23(1):12–31.
15. FoodData Central. United States Department of Agriculture Agricultural Research Service [Internet]. 2019. <https://fdc.nal.usda.gov/>
16. Fracanzani AL, Conte D, Fraquelli M, Taioli E, Mattioli M, Losco A, Fargion S. Increased cancer risk in a cohort of 230 patients with hereditary hemochromatosis in comparison to matched control patients with non-iron-related chronic liver disease. *Hepatology.* 2001;33(3):647–651.
17. Gill RM, Kakar S. Liver and gallbladder. In: Kumar V, Abbas AK, Aster JC (eds.). *Robbins & Cotran Pathologic Basis of Disease.* 10th ed. Philadelphia (PA): Elsevier; 2021. p. 823–879.
18. Josefsen TD, Sørensen KK, Mørk T, Mathiesen SD, Ryeng KA. Fatal inanition in reindeer (*Rangifer tarandus tarandus*): Pathological findings in completely emaciated carcasses. *Acta Vet Scand.* 2007;49(27):1–11.
19. Kew MC. Hepatic iron overload and hepatocellular carcinoma. *Liver Cancer.* 2014;3(1):31–40.
20. Kleiner DE, Chalasani NP, Lee WM, Fontana RJ, Bonkovsky HL, Watkins PB, Hayashi PH, Davern TJ, Navarro V, Reddy R, Talwalkar JA, Stolz A, Gu J, Barnhart H, Hoofnagle JH. Hepatic histological findings in suspected drug-induced liver injury: systematic evaluation and clinical associations. *Hepatology.* 2014; 59(2):661–670.
21. Korine C, Arad Z. Effect of water restriction on temperature regulation of the fruit-bat *Rousettus aegyptiacus*. *J Therm Biol.* 1993;18(2):61–69.
22. Kurta A, Bell GP, Nagy KA, Kunz TH. Water balance of free-ranging little brown bats (*Myotis lucifugus*) during pregnancy and lactation. *Can J Zool.* 1989;67(10):2468–2472.
23. Lavin SR, Chen Z, Abrams SA. Effect of tannic acid on iron absorption in straw-colored fruit bats (*Eidolon helvum*). *Zoo Biol.* 2010;29(3):335–343.
24. Leone AM, Crawshaw GJ, Garner MM, Frasca S, Stasiak I, Rose K, Neal D, Farina LL. A retrospective study of the lesions associated with iron storage disease in captive Egyptian fruit bats (*Rousettus aegyptiacus*). *J Zoo Wildl Med.* 2016;47(1):45–55.
25. Lowenstine LJ, Stasiak IM. Update on iron overload in zoologic species. In: Miller RE, Fowler ME (eds.). *Fowler's Zoo and Wild Animal Medicine, Volume 8.* St. Louis (MO): Elsevier; 2015. p. 674–681.
26. Mandishona E, MacPhail AP, Gordeuk VR, Kedda MA, Paterson AC, Rouault TA, Kew MC. Dietary iron overload as a risk factor for hepatocellular carcinoma in Black Africans. *Hepatology.* 1998;27(6):1563–1566.
27. Mayer AM. Historical changes in the mineral content of fruits and vegetables. *Br Food J.* 1997;99(6):207–211.
28. McKnight CA, Wise AG, Maes RK, Howe C, Rector A, Van Ranst M, Kiupel M. Papillomavirus-associated basosquamous carcinoma in an Egyptian fruit bat (*Rousettus aegyptiacus*). *J Zoo Wildl Med.* 2006;37(2):193–196.

29. McLelland DJ, Dutton CJ, Barker IK. Sarcomatoid carcinoma in the lung of an Egyptian fruit bat (*Rousettus aegyptiacus*). *J Vet Diagn Invest*. 2009;21(1):160–163.
30. McLuckie AJ, Barrs VR, Lindsay S, Aghazadeh M, Sangster C, Beatty JA. Molecular diagnosis of *Felis catus* gammaherpesvirus 1 (FcaGHV1) infection in cats of known retrovirus status with and without lymphoma. *Viruses*. 2018;10(3):128.
31. Munday JS, Löhr CV, Kiupel M. Tumors of the alimentary tract. In: Meuten DJ (ed.). *Tumors in domestic animals*. 5th ed. Ames (IA): John Wiley & Sons, Inc; 2017. p. 499–601.
32. National Institutes of Health Office of Dietary Supplements. Vitamin C: fact sheet for health professionals. National Institutes of Health Office of Dietary Supplements [Internet]. 2021. <https://ods.od.nih.gov/factsheets/VitaminC-HealthProfessional/>
33. Niederau C, Fischer R, Pürschel A, Stremmel W, Häussinger D, Strohmeyer G. Long-term survival in patients with hereditary hemochromatosis. *Gastroenterology*. 1996;110(4):1107–1119.
34. Olds JE, Burrough ER, Fales-Williams AJ, Lehmkuhl A, Madson D, Patterson AJ, Yaeger MJ. Retrospective evaluation of cases of neoplasia in a captive population of Egyptian fruit bats (*Rousettus aegyptiacus*). *J Zoo Wildl Med*. 2015;46(2):325–332.
35. Olds JE, Derscheid RJ. Extraskelletal osteosarcoma in an Egyptian fruit bat (*Rousettus aegyptiacus*). *Vet Rec Case Rep*. 2018;6(2):e000579.
36. Paganoni R, Lechel A, Vujic Spasic M. Iron at the interface of hepatocellular carcinoma. *Int J Mol Sci*. 2021;22(8):4097.
37. Rasche A, Souza BFCD, Drexler JF. Bat hepadnaviruses and the origins of primate hepatitis B viruses. *Curr Opin Virol*. 2016;16:86–94. [10.1016/j.coviro.2016.01.015](https://doi.org/10.1016/j.coviro.2016.01.015).
38. Siegal-Willott J, Heard D, Sliess N, Naydan D, Roberts J. Microchip-associated leiomyosarcoma in an Egyptian fruit bat (*Rousettus aegyptiacus*). *J Zoo Wildl Med*. 2007;38(2):352–356.
39. Stasiak IM, Smith DA, Crawshaw GJ, Hammermueller JD, Bienzle D, Lillie BN. Characterization of the hepcidin gene in eight species of bats. *Res Vet Sci*. 2014;96(1):111–117.
40. Stasiak IM, Smith DA, Ganz T, Crawshaw GJ, Hammermueller JD, Bienzle D, Lillie BN. Iron storage disease (hemochromatosis) and hepcidin response to iron load in two species of pteropodid fruit bats relative to the common vampire bat. *J Comp Physiol B*. 2018;188(4):683–694.
41. Stewart AB, Dudash MR. Foraging strategies of generalist and specialist Old World nectar bats in response to temporally variable floral resources. *Biotropica*. 2018;50(1):98–105.
42. Tang Z, Sheng L, Cao M, Liang B, Zhang S. Diet of *Cynopterus sphinx* and *Rousettus leschenaulti* in Xishuangbanna. Shou Lei Xue Bao [Acta Theriologica Sinica]. 2005;25(4):367–372.
43. Van der Westhuyzen J. Haematology and iron status of the Egyptian fruit bat, *Rousettus aegyptiacus*. *Comp Biochem Physiol A Comp Physiol*. 1988;90(1):117–120.
44. Van Nguyen D, Van Nguyen C, Bonsall D, Ngo TT, Carrique-Mas J, Pham AH, Bryant JE, Thwaites G, Baker S, Woolhouse M, Simmonds P. Detection and characterization of homologues of human hepatitis viruses and pegiviruses in rodents and bats in Vietnam. *Viruses*. 2018;10(3):102.
45. Wadsworth PF, Jones DM, Pugsley SL. Hepatic haemosiderosis in birds at the Zoological Society of London. *Avian Pathol*. 1983;12(3):321–330.
46. Wang B, Yang XL, Li W, Zhu Y, Ge XY, Zhang LB, Zhang YZ, Bock CT, Shi ZL. Detection and genome characterization of four novel bat hepadnaviruses and a hepevirus in China. *Virol J*. 2017;14:40. [10.1186/s12985-017-0706-8](https://doi.org/10.1186/s12985-017-0706-8).
47. Wilson DW. Tumors of the respiratory tract. In: Meuten DJ (ed.). *Tumors in domestic animals*. 5th ed. Ames (IA): John Wiley & Sons, Inc; 2017. p. 467–498.
48. Zadrozny LM, Williams CV, Remick AK, Cullen JM. Spontaneous hepatocellular carcinoma in captive prosimians. *Vet Pathol*. 2010;47(2):306–311.

*Accepted for publication 2 October 2023*

**Supplementary Table 1.** Primers used for pan-hepadnavirus PCRs.